

Validation Platform for Development of Computational Fluid Dynamics of Intra-Cardiac Blood-Flow

Rasmus Hvid, Jørgen Arendt Jensen, Matthias Bo Stuart and Marie Sand Traberg
Center for Fast Ultrasound, Department of Health Technology, Technical University of Denmark
2800 Kgs. Lyngby, Denmark

Abstract—This study is an initial evaluation of a validation platform for computational fluid dynamics (CFD) pipelines made for human intra-cardiac flow estimation. The pipelines use image-based prescribed geometry CFD from computed tomography angiography (CTA). In this study the CTA provides approximately 20 volumetric images within one cardiac cycle. The validation platform consists of a dynamic heart phantom which mimics the human heart in CTA and ultrasound (US) measurements. The flow inside the phantom right ventricle (RV) was measured using two methods: 1) a novel CFD pipeline applied using the CTA data (3D+time). 2) US vector flow imaging (VFI) measured directly on the phantom (2D+time). The CFD and VFI are compared quantitatively by comparing point evaluations (line averages) of the in-plane fluid velocity magnitude. The similarity of the line averages, assessed from plots, is found to be depending on the spatial position of the lines. Some positions are very similar in CFD and VFI and some are not. Furthermore a qualitatively comparison is made by plotting the corresponding 2D slices of the vector fields which confirms the quantitative assessment: the overall flow patterns are similar but not everywhere.

I. INTRODUCTION

Intra-cardiac flow patterns have the potential to become an important metric in diagnosis and treatment of cardiovascular diseases in future medicine [1]. Currently the gold standard for estimating intra-cardiac flow patterns is magnetic resonance imaging (MRI) which has several drawbacks including price, acquisition time and relatively poor spatial resolution [2]. An alternative to MRI is ultrasound with the downside of practicality: it is hard to obtain a good signal through the surrounding tissue [3]. Lately image-based computational fluid dynamics (CFD) has realistically been competing in the field of patient-specific intra-cardiac flow estimation by offering the potential of better spatial and temporal resolution [4]. Here an expandable validation platform is demonstrated by presenting a validation of a CFD pipeline.

II. METHODS

The velocity fields (blood flow patterns) in a dynamic heart phantom are estimated using two methods and the results are compared. The methods are CFD and VFI. For the purpose of this study the phantom movement is simplified to a cyclic compression. Because the programmed phantom movement has no beat-to-beat variation the inter-measurement variation is

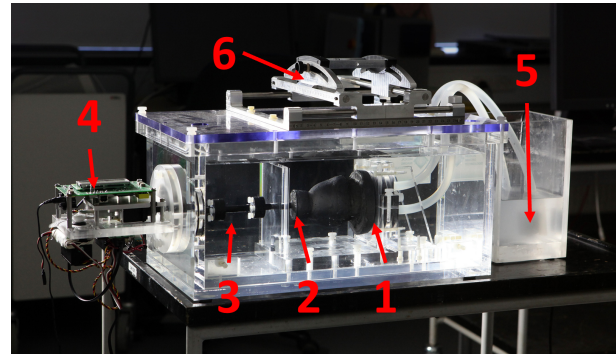


Fig. 1. Dynamic heart phantom (DHP) from Shelley Medical Imaging Technologies. 1: PVA base 2: PVA apex 3: Actuator rod 4: Servo motors and micro controller 5: Blood-mimicking fluid reservoir 6: Fixture for US probe where angle and position can be adjusted

minimal. The CFD pipeline applied has not been described in the literature yet and is therefore presented in this paper.

A. Dynamic heart phantom setup

The phantom is a dynamic bi-ventricular heart phantom (DHP) from Shelley Medical Imaging Technologies (Toronto, Canada). The phantom has no heart valves. The phantom ventricles are made of polyvinyl alcohol (PVA) with additives. The additives make the ventricles appear as myocardium on computed tomography (CT) and ultrasound (US). The PVA heart is submerged in a water-filled tank and anchored at the base. Attached to the heart apex is an actuator rod which is attached to a servo motor. The servo motor is controlled from a programmable micro-controller. The micro-controller has three default output channels: compression, torsion and electrocardiography (ECG) output. The ECG output is used for synchronizing medical imaging. In this study only the right phantom ventricle is measured and simulated.

1) *Phantom Flow*: A constant inlet flow is applied through the right ventricle by a pump submerged in a reservoir of blood mimicking fluid. The flow rate is ≈ 5 L/min. See Fig. 1.

2) *Phantom Movement*: The movement programmed onto the micro-controller has three channels: compression, torsion

TABLE I
PHANTOM MOVEMENT SUMMARIZED

Function name	Function expression
Flow(t)	5l/min
Compression(t)	$\sin(\pi t/T)^2 \cdot \maxDisp$
Torsion(t)	0°
ECG(t)	$\begin{cases} 1 & \text{if } (n \cdot T) \leq t \leq (n \cdot T + 0.1s) \\ 0 & \text{otherwise} \end{cases}$
for	$n = 0, 1, \dots, N_{cycles}$ $T = 0.8s$

and ECG output. Furthermore the flow rate can be programmed as a fourth channel. For the simplified movement in this study two channels were used: compression and ECG output. The compression follows a squared sine function with 14mm amplitude and a frequency of 75 beats per minute (similar to Fig. 2). The ECG was programmed as a narrow rect function. The functions are summarized in table I where T is the cardiac cycle period and \maxDisp is the maximum displacement of the heart phantom apex.

B. Geometry

The geometry used for the simulation is a segmentation of a Computed Tomography Angiography (CTA) scan of the heart phantom.

1) *Computed tomography*: A CTA was performed on the phantom using a Canon (TOSHIBA) Aquilion ONE scanner. The cardiac cycle is defined as the R-R interval on the ECG and split into 20 phases corresponding to 5% increments (from 0% to 95%). The spatial resolution of the CTA reconstruction used for this study results in a voxel size of $(x, y, z) = (0.6, 0.6, 0.5)mm^3$ with no overlap. The temporal resolution is 20 phases per heart cycle which results in a sample period of $0.8s/20 = 0.04s$. This corresponds to a volume rate of 25Hz. Contrast fluid was added to the blood mimicking fluid before the CTA. The contrast fluid increases the contrast between blood and surrounding tissues which eases segmentation. This is the same procedure as for in-vivo CTA.

2) *Moving fluid domain*: The fluid domain is defined by an imported surface mesh from segmentation of the CTA. The 80% phase (frame #17 out of 20) where the phantom compression is minimal is used for this study. The movement is prescribed to this surface by a simplified linear deformation exclusively in the z-direction and a maximum displacement at the apex of 10mm ($zDisp$ in (2)). Note that 10mm displacement of the fluid domain's apex roughly corresponds to a 14mm displacement of the PVA's apex. The volumetric mesh nodes are smoothed corresponding to the surface movement. The simplified prescribed movement is verified by comparing the deformed geometry with the respective CTA segmentation in plots.

C. Computational fluid dynamics

The CFD pipeline is solved numerically in COMSOL Multiphysics v5.4 (COMSOL AB Stockholm, Sweden). Here the

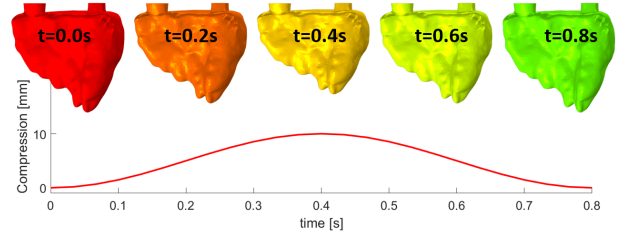


Fig. 2. Illustration of the fluid domain (right ventricle) surface compression. **Top**: RV surface at $t=0[s]$, $0.2[s]$, $0.4[s]$, $0.6[s]$, $0.8[s]$. **Bottom**: Compression of the RV apex over 1 cycle (see (2))

incompressible Navier-Stokes equations

$$\rho \left(\frac{\partial \vec{u}}{\partial t} + (\vec{u} \cdot \nabla) \vec{u} \right) = -\nabla p + \eta \nabla^2 \vec{u} \quad (1)$$

$$\nabla \cdot \vec{u} = 0$$

are solved numerically assuming isothermal laminar flow. The blood mimicking fluid is assumed to be Newtonian.

In (1) \vec{u} is the fluid velocity vector (m/s), t is time (s), p is pressure (Pa), $\rho = 1060kg/m^3$ is the fluid density and $\eta = 3.5mPa \cdot s$ is the fluid viscosity. ∇ is the del operator and ∇^2 is the Laplace operator.

1) *Studies*: The simulation is split into several studies to save computational resources and making the simulation solutions more stable.

Study 1: mesh movement

This study solves the spatial position of every mesh node for a single cycle. The movement is prescribed to the *wall* (see Fig.3) as a displacement function (see (2)). The function is periodic, so the mesh nodes on the *wall* will always end exactly where they started. The positions of the mesh nodes inside the fluid domain is computed using Yeoh smoothing. The position and velocity of each mesh node are stored between $t=0s$ and $t=0.8s$ for each timestep of $\Delta t=0.01s$. These positions are re-used in all of the subsequent cycles (studies 3-8).

$$dz(Z, t) = \frac{z}{lHeart} zDisp \cdot \sin \left(\frac{t\pi}{T} \right)^2 \quad (2)$$

in (2) (x, y, z) are coordinates in the spatial frame of reference and (X, Y, Z) are coordinates in the material frame of reference. $T=0.8s$ is the time period, $lHeart=60mm$ is the approximate length of the RV-cavity and $zDisp=10mm$ is the maximum displacement at the RV-cavity apex.

Study 2: initial conditions for first cycle

The choice of initial conditions has a great influence on how fast the solution converges. Poorly chosen initial conditions can make a model solution unstable and even unsolvable. Therefore instead of applying inlet flow on "zero pressure, zero velocity" initial conditions, the inlet flow is ramped up from 0 L/min to

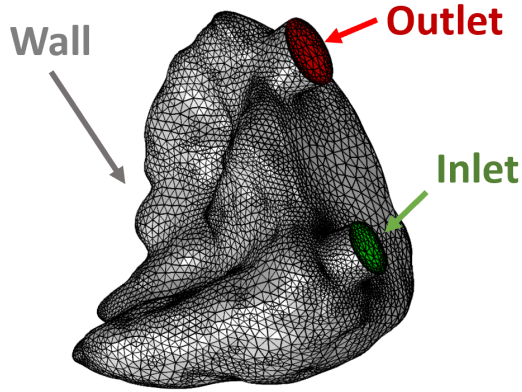


Fig. 3. Surface mesh (mesh size: "Normal") of the phantom right ventricle. The boundary types are collared: **Gray:** Wall **Green:** Inlet **Red:** Outlet

5 L/min over a time period of ≈ 0.8 s. The outlet is defined as constant pressure $p=0$ Pa. In this study the wall is stationary in the $t=0$ s configuration from Study 1. The boundary condition on the wall is zero slip which in the stationary geometry corresponds to $\vec{u}=0$ at the wall. The time stepping is free, and only the last time frame is saved.

Study 3: cycle 1

This study computes the CFD of the moving geometry nodes (from study 1) using the initial conditions calculated in the previous study: study 3 uses the last time step of Study 2 as initial conditions. The boundary conditions are as follows:

Inlet Fully developed, constant inlet flow (5 L/min).

Outlet Normal flow, zero pressure.

Wall Zero slip: $\vec{u}_{fluid} = \vec{u}_{wall}$ at the wall.

Study 4: cycle 2

Same study type as study 3 except the initial conditions for study 4 is the last time frame from study 3. This procedure is followed for as many subsequent cycles necessary. The simulation is run for up to 6 cycles, or until the solution is converging towards the same periodic flow field. The solution in this paper is the 6th cycle repeated.

TABLE II
CFD KEY NUMBER AND RESOURCES

Boundary elements	13 878
Total elements	152 512
Computation time	1h 18m 7s
Resources for 8 studies (6 cycles)	2x Intel Xeon CPU E5-2660 v3 2 sockets, 20 cores, 2.60 GHz Available memory: 128.65 GB

2) *Meshing*: COMSOL has a built in automatic mesh function with a set of 9 pre-defined sizes (extremely coarse to extremely fine) which takes into account the type of physics

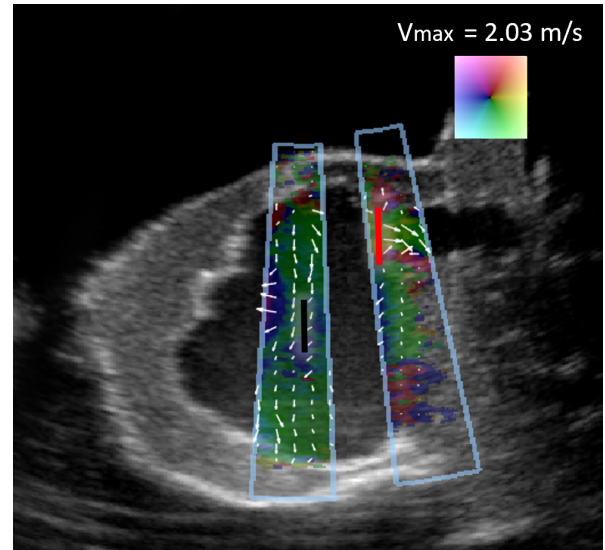


Fig. 4. A B-mode US image with VFI overlay from two separate acquisition. All three are from the 0% cardiac phase at minimum compression.

solved for. In this simulation the physics is "fluid dynamics". In previous work [5] solutions from the mesh sizes "fine" and "normal" are within 2% in a mesh independence study. The mesh size for this study has been set to "normal" based on this. The mesh (surface elements only) is plotted in Fig. 3.

D. Vector Flow Imaging

VFI is measured using a modified BK5000 scanner and a 6C2 convex array probe (BK Medical, Herlev DK) mounted in a sliding fixture for capturing multiple parallel planes with 5mm intervals. Several acquisitions are made of each plane to obtain a higher frame rate. For full area flow estimations the frame rate is only ≈ 4 Hz, for smaller areas of flow estimation the frame rate is ≈ 16 Hz which is more appropriate for capturing the intra cardiac fluid dynamics. Examples of the smaller areas of VFI are seen in figure 4.

III. RESULTS

A. Qualitative comparison

Initially the vector fields are compared qualitatively slice by slice. This is done by visual comparison of 2D+t vector fields. The overall flow patterns are found to be similar, but with variations. See figure 5.

B. Quantitative comparison

Several one-dimensional and time-dependent metrics are extracted from the estimations and compared. These metrics are point evaluations and "line averages". The line average is a better suiting metric to compensate for the roughly estimated co-registration in this study. In this paper two line averages are shown for 5 cycles. See Fig. 4, 5(a) and 6.

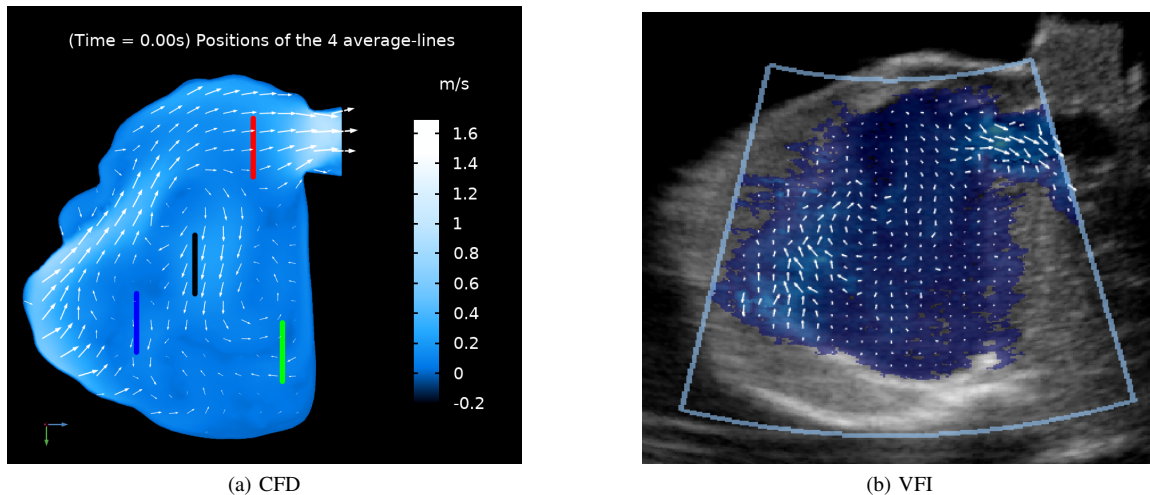


Fig. 5. **a:** Slice from CFD. Colorbar is in-plane velocity magnitude. The average lines plotted in Fig. 6 is marked in red and black respectively. **b:** VFI of the same slice approximately at the same phase of the cardiac cycle.

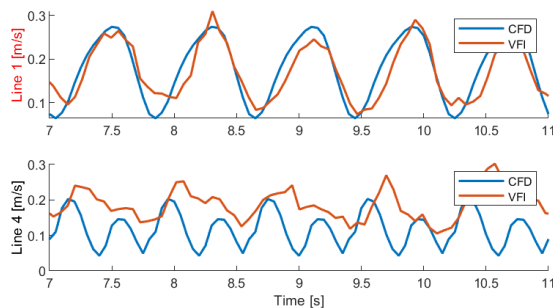


Fig. 6. Line averages of the in-plane velocity magnitude from images in Fig. 4 and 5(a)

IV. DISCUSSION

Finding a suitable metric for validating a complex flow in 3D+time is not an easy task. In this study some points/lines have been selected, but a more global evaluation is preferable for validation purposes. As the simulation model is still being developed any mismatch between the VFI and CFD might be because of a CFD error.

A. Limitations/considerations

The valve-less phantom flow is not directly comparable to the in-vivo flow. The accuracy of the prescribed movement has not been verified. In future CFD pipelines, volumetric image registration will be used to estimate the wall movement directly. Co-registration has not been done precisely for this initial study although the validation setup has the potential for precise co-registration. Furthermore the inlet and outlet tubes have been cut relatively close to the phantom geometry. The effects of this has not yet been investigated.

V. CONCLUSION

To test the feasibility of further developing a phantom based validation platform the phantom intra-ventricular flow dynamics were measured using two methods. The methods show similarities both qualitatively, by visual comparison of slices, and quantitatively by comparing time dependent point evaluations of the velocity field.

ACKNOWLEDGMENT

The authors would like to thank Klaus F. Kofoed (MD, Ph.D, DmSc Department of Cardiology, Rigshospitalet, University of Copenhagen) for making the CTA data acquisition possible.

REFERENCES

- [1] L. Zhong, J. Zhang, B. Su, R. Tan, J. Allen, and G. Kassab, "Application of patient-specific computational fluid dynamics in coronary and intra-cardiac flow simulations: Challenges and opportunities," *Frontiers in Physiology*, pp. 1–17, 2018. [Online]. Available: <https://www.scopus.com/inward/record.uri?eid=2-s2.0-85049077345&doi=10.3389%2ffphys.2018.00742&partnerID=40&md5=4c7aec16a50d126dbb2224d5fcc660a9>
- [2] S. Doost, D. Ghista, B. Su, L. Zhong, and Y. Morsi, "Heart blood flow simulation: A perspective review," *BioMedical Engineering Online*, vol. 15, no. 1, pp. 1–28, 2016. [Online]. Available: <https://www.scopus.com/inward/record.uri?eid=2-s2.0-84983672153&doi=10.1186%2fs12938-016-0224-8&partnerID=40&md5=22ec6a808d0a106530db8e333ed843db>
- [3] D. Munoz, M. Markl, J. Mur, A. Barker, C. Fernandez-Golfin, P. Lancellotti, and J. Gomez, "Intracardiac flow visualization: Current status and future directions," *European Heart Journal Cardiovascular Imaging*, vol. 14, no. 11, pp. 1029–1038, 2013. [Online]. Available: <https://www.scopus.com/inward/record.uri?eid=2-s2.0-84885928303&doi=10.1093%2fahj/cjz086&partnerID=40&md5=bfd090b6ef9544b333672c373b3db31>
- [4] J. Lantz, L. Henriksson, A. Persson, M. Karlsson, and T. Ebbens, "Patient-specific simulation of cardiac blood flow from high-resolution computed tomography," *J. Biomech. Eng.*, vol. 138, pp. 121004–1–121004–9, 2016.
- [5] R. Hvid, "Development of 3d simulation model of the heart for validation of vector flow imaging," MSc Thesis, Technical University of Denmark, 2018.